# LOAD PARTITIONING IN ZR-2.5%NB DURING COMPRESSION

S. Cai[1,a], M.R. Daymond[1,b], R. Holt[1,c] and E.C. Oliver[2,d]

[1]Department of Mechanical and Materials Engineering, Queen's University,
Kingston, ON, K7L 3N6, Canada.
[2]ISIS, Rutherford Appleton Lab., Didcot, OX11 0QX, UK
[a]1sc12@qlink.queensu.ca, [b]daymond@me.queensu.ca, [c]holt@me.queensu.ca, [d]e.c.oliver@rl.ac.uk

Keywords: interphase, intergranular, residual stress/strain, Neutron diffraction, TOF, Zr-2.5Nb

**Abstract.** A series of TOF neutron diffraction in-situ uniaxial compression tests have been carried out on textured Zr-2.5Nb. Test samples were prepared from the hot rolled plate with a moderate texture where the basal plane normal is mainly distributed between the transverse (TD) and plate normal (ND) directions. In a set of tests, load was applied along each of the three principle directions, and the evolution of the lattice strain was also measured in these directions. The intergranular strain was monitored by single peak fits while the interphase strain was obtained by Rietveld refinements. Results show that the load sharing changes between the α- and β–phases at various macroscopic applied loads. The α-phase yields first and then takes a smaller load increment for increasing macroscopic stress. The β–phase yields at a higher applied stress and the load is then transferred back to the α-phase. Load partitioning also occurs between differently oriented grain families in each phase. This load partitioning produces residual interphase and intergranular stresses in Zr-2.5Nb. The average residual phase stress is low in the α-phase, however, the intergranular stresses can be significant.

## Introduction

Used in pressure tubes in the CANDU power generation system [1], the mechanical properties of Zr-2.5Nb have attracted researchers for many years [2-6]. Models have been established to predict the material's in-situ behavior [2-4]. However, most of this work has focused on the irradiation growth or creep behavior [2-4]. In particular the contribution of various slip systems or relative contributions of the two phases to the deformation of Zr-2.5Nb has not been thoroughly studied. Indeed, most of the studies to date have ignored the cubic β–phase because of its relatively small volume fraction and have treated the material as a single phase polycrystal [2,3,5] with the aim of ignoring any related error by fitting to experimental data. However, recent studies [5,6] have demonstrated that the overall properties of Zr-2.5Nb are highly dependent on the properties and the distribution (both geometric and texture) of the β–phase. Neglecting the β–phase is likely to introduce significant errors in modeling the deformation response of the overall material [6]. Our project is to study the influence of the β–phase on the deformation mechanisms of this material.

The internal stresses generated during deformation in multiphase materials can be considered to consist of interphase stresses, which are due to the variation in mechanical properties between phases, and intergranular stresses, which are caused by the differing mechanical response of differently orientated grains [7]. In recent years, neutron diffraction has been used to measure the evolution of both types of stresses because of its ability to probe the strain response of bulk material [8-10]. At most reactor neutron sources, a monochromatic neutron beam is directed onto the sample and the diffracted neutrons are recorded at scattering angles which correspond to groups of grains in the polycrystal which have particular orientations, according to Bragg's law. The *average* phase applied stress-internal strain behavior is taken to be that of grain orientationss in the phase whose stress and lattice strain curves remain more or less linear even when plasticity is extensive [8]. In the time of flight (TOF) technique, a pulsed white beam is used. The diffraction from different orientations of grains is determined by the time for the neutron to reach the detector [11]. While the lattice strains of individual grain families can be monitored from the shift of their individual peak positions, it is common practice to define the average phase strains by fitting the whole spectrum simultaneously using a multiphase Rietveld refinement [12-13].

As part of our larger project, this paper describes preliminary results of experiments where the evolution of interphase and intergranular strains developed in Zr-2.5Nb during compression was studied by TOF neutron diffraction.

## Materials and experimental method

The compositions of the experimental material was 2.5wt% Nb, 900-1600ppm O, 1500ppm Fe, 400ppm C and balance Zr. Ingots were forged to 4 inches thick at 1065°C and then hot rolled to 2 inches thick at about 700°C and air cooled to room temperature. Samples of size Ø8mm×16mm were cut out from the rolled plate with the cylinder axial parallel to the rolling (RD), transverse (TD) or plate normal direction (ND). While all three principal strains were determined for all three loading directions, due to lack of space only some of the data is shown here. The microstructure is shown in Figure 1. It can be seen that the predominant *hcp* α-grains have a plate-like shape with length and width about 30μm and thickness around 3μm, giving an aspect ratio about 10 to 1. The *bcc* β–phase, with volume fraction of about 12%, is distributed between the α grains.

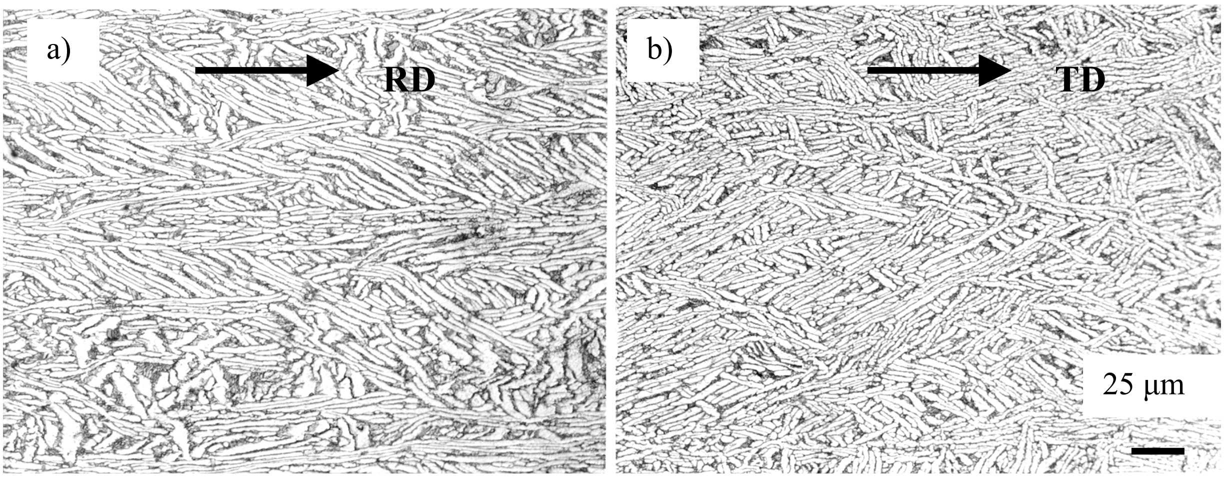


Figure 1 Microstructure of Zr-2.5Nb samples looking from the transverse direction a) and rolling direction b).

Figure 2 shows that the material has a weaker texture than that seen in typical extruded CANDU pressure tubes [5]. The α–phase has its basal plane normal mostly orientated towards TD and ND, while the β–phase has its (100) plane normal weakly distributed along ND. The resolved fractions of basal plane normal in rolling, transverse and normal direction ($f_R$, $f_T$ and $f_N$) are 0.27, 0.39 and 0.34 [14].

In-situ neutron diffraction lattice strain measurements were carried out during uniaxial compression on ENGIN-X at the ISIS pulsed neutron facility, Rutherford Appleton Laboratory, UK. The loading axis is horizontal and at $45^0$ to the incident beam. Two detector banks are set up horizontally and at angles $\pm 90^0$ to the incident beam, allowing simultaneous measurement of lattice strains in directions both parallel and perpendicular to the applied load [15]. More details can be found in [16]. A series of increasing compressive loads were applied along the axial direction to produce a final true strain of ~10%. The sample strain was kept constant during the time taken for the neutron measurement. Unload/reload events were performed in the plastic region to measure the evolution of residual strain as a function of plastic strain. An average counting time of about 20 minutes was used for each applied strain. The macroscopic strain was monitored on the samples using a dynamic extensometer clip gauge. The incident beam was 8 mm high and 4 mm wide, the radial collimators in use provided a scattered aperture of 4 mm.

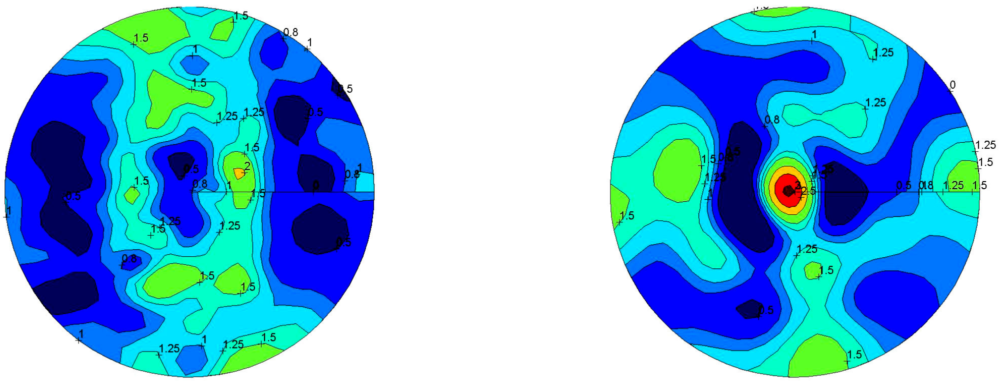

Figure 2 Pole figures of a) α−phase basal plane and b) β−phase (100) plane. ND is in the center, TD is vertical and RD is horizontal.

## Results and Discussions

**Macroscopic response.** Figure 3 shows the macroscopic stress strain behavior obtained in the three testing directions. The ND and TD samples have a similar mechanical response to each other, with Young's modulus ~100GPa and yield stresses $\sigma_{0.2}$ ~430MPa and ~420MPa respectively. The Young's modulus of the RD sample is ~86GPa and $\sigma_{0.2}$ ~350MPa. The anisotropic properties of *hcp* polycrystalline materials are mainly determined by the orientation of the c-axis. It is thus not surprising that the TD and ND samples, which have larger resolved fraction of basal plane, have a higher yield strength than RD sample. A similar relationship between strength and texture was found in [5]. The work hardening rate is similar for all the three test directions.

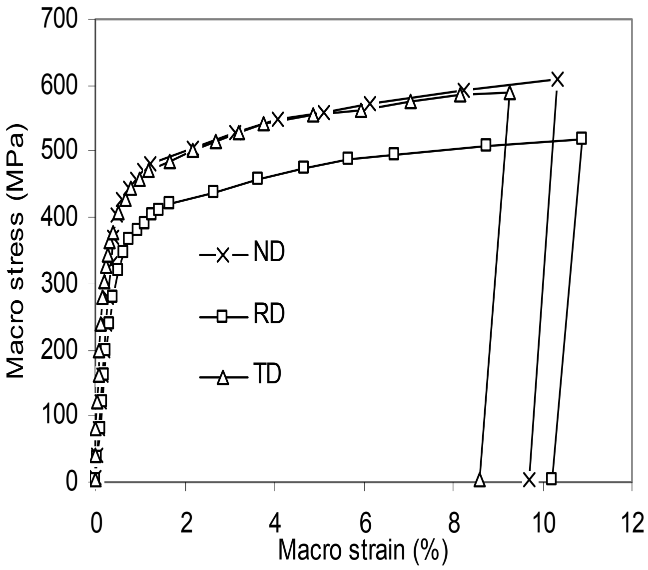


Figure 3 The macroscopic response of samples testing from three directions. The stress and strain are reversed to positive for convenience.

**Evolution of interphase strain**. Figure 4 shows examples of neutron diffraction spectra prior to deformation acquired from two directions. The stronger α−basal texture in ND direction is shown in Fig. 4a) corresponding a strong [10-10] distribution in RD direction (Fig. 4b). A weak β−(110) texture can be seen in the ND direction. Fig 4a) also shows the result of a conventional two-phase Rietveld refinement [12,13], while Fig. 4b) shows the result of independent peak fitting [12,13]. Despite their different principles, it can be seen that both methods fit the experimental data very well at this zero load. While as the load increase, the error between Rietveld fit and experimental data will increase due to the plasticity anisotropy of the α−phase.

The elastic phase strains measured parallel and perpendicularto the applied stress, as determined by a conventional two-phase Rietveld refinement [12,13], are plotted as a function of applied stress in Fig. 5. The average strain in the α−phase is calculated as $(2\varepsilon_a+\varepsilon_c)/3$; this has been shown to be a good approximation to the mean phase strain in the case of near random textures [13]. The measured yield stress determined is also shown in Fig. 5 by dashed line. Since the material has a

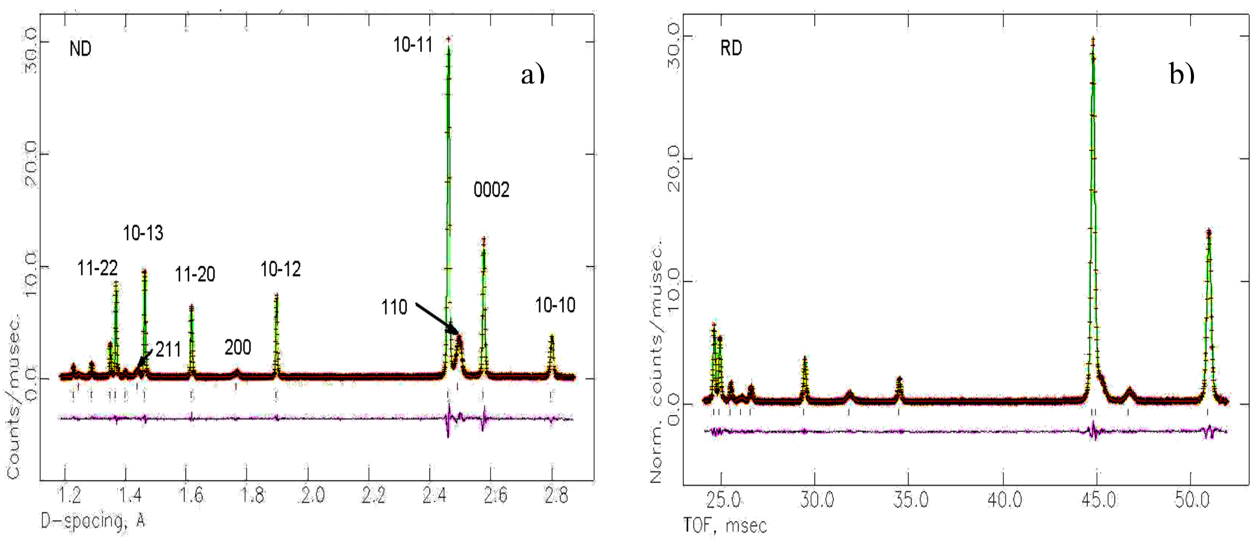


Figure 4 Neutron diffraction spectra of one of the samples from a) ND direction and b) RD direction. The upper part of each plot shows the experimental and fitted results. The second line in each plot is the residual of the fitting.

weak texture and the coefficients of thermal expansion of these two phases are close (a-α: $5.7\times10^{-6}$/K, c-α: $10.3\times10^{-6}$/k; β: $7.4\times10^{-6}$/K [17]), any residual stresses at the start point are small and neglected here. The reference lattice parameters are thus taken as those at the start of loading. In all cases, the phase response below the yield stress is linear. The slope of the stress and strain curves indicates the relative stiffness of these two phases, while the ratio of the parallel to perpendicular slope gives the Poission's ratios, which are ~0.33 for both phases.

Deviations from linearity are observed in the phase strains of all three samples at macro-stresses close to the macroscopic yield points. The lattice strains in the α- phase in the direction parallel to the applied load shifts towards tension relative to the linear elastic line, while the compressive strains in the parallel direction β-phase increase, indicating yield of the α-phase and a load transfer towards the β-phase. Since the α is the predominant phase, its' yielding corresponds to large scale plasticity of the sample. The gradient of the parallel direction β-phase after the yield is shallower than before. This indicates that the β-phase bears an increasing part of the applied load while the proportion of the load taken by the α-phase is decreasing with the plastic flow. The amount of the change in strain of the β-phase at a given stress is much larger than that in the α- phase; this is due to the small volume fraction and smaller stiffness of the β-phase. A second shift is seen in the β res-

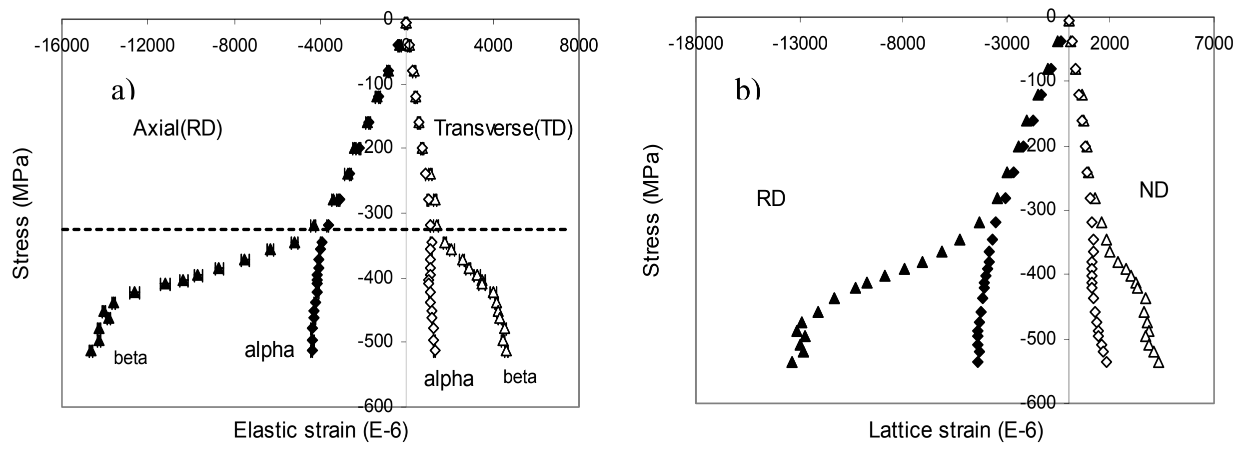


Figure 5 lattice phase strains determined by Rietveld fitting as a function of compressive stress: a) RD sample, transverse is TD; b) RD sample, transverse is ND. Dash lines show the 0.2% offset yield stress. The average error is ~$20\text{-}40\times10^{-6}$ for α–phase and ~$80\text{-}120\times10^{-6}$ for β–phase.

ponse in the RD sample at a load of about ~430MPa. The parallel direction β strain shifts back, indicating yield of the β phase, the load shared by the α-phase then increases, producing a slight increase in the lattice strain. A similar observation can be made at ~500MPa in the TD and ND samples.

A behavior corresponding to the Poisson response is observed in the direction perpendicular to the applied load. The α-phase shows deviation from linearity at the same applied stresses as seen in the parallel direction. Again at higher applied stresses, the yield of the β-phase causes a second inflection.

Comparison between Fig. 5a) and 5b) shows that when the applied load is in the RD, the responses in TD and ND perpendicular to the applied load are very similar, which again is due to their similar basal plane distributions. Thus only the results of one perpendicular direction (the TD) are given below.

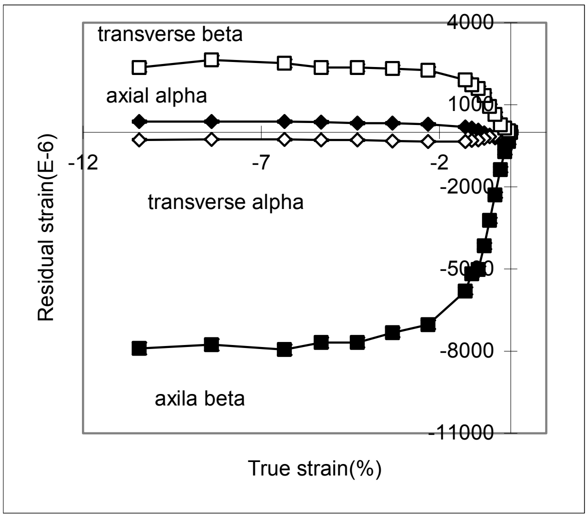


Figure 6 Development of residual phase strain during deformation in RD sample, transverse is TD. The average error is ~20-40×$10^{-6}$ for α−phase and ~80-120×$10^{-6}$ for

Fig. 6 plots the evolution of residual stresses versus macroscopic strain of the RD sample. It can be seen that the residual strain in both phases increases rapidly at the beginning of plasticity and then reaches a steady state in the higher strain region. The saturated residual strain is about ~400-450×$10^{-6}$ in the axial direction for the α-phase and ~6000-8000×$10^{-6}$ in axial direction for the β-phase. The corresponding values are ~250-300×$10^{-6}$ and ~2500×$10^{-6}$ in the TD perpendicular to the applied load and ~150×$10^{-6}$ and ~2000×$10^{-6}$ for ND perpendicular to the applied load., This gives a β to α strain ratio about 10-15 in all three directions, and Poisson ratios of about a third to a half for both phases. The differences between TD and ND strains, compared to the strains in the RD parallel to the applied load indicate a moderate axial asymmetry during plasticity, due to the texture. The relative magnitude of residual strains seen in the β−phase, compared to those in the α−phase, is somewhat larger than would be expected based on simple volume fraction assumptions.

**Evolution of intergranular strain.** The evolutions of lattice strains in directions both parallel and perpendicular to the applied load for selected grain families – as obtained by single peak fits - are plotted in Figure 7. The macroscopic 0.2% yield stress is also shown by a dashed line. Small elastic anisotropy is seen for both phases in both parallel and perpendicular directions, while a significant plastic anisotropy is observed once the applied stress is close to the macroscopic yield stress.

Based on the single crystal properties of the α−phase, it is not surprising that in Zirconium alloys the {0002} grain family has the largest elastic stiffness, as confirmed by Fig.7 a. However, due to the constraint from the β−phase and other grain families in the α-phase, the elastic anisotropy is not as large as that seen in the single crystal. In the direction parallel to applied load, it can be seen that the {10-10} and {11-20} grain families show yield first at stresses ~300MPa, and transfer load to other orientations - their lattice strains shift back towards tension from the linear elastic line. Then grain orientations {10-11}, {10-12} and {10-13} yield in sequence at applied stresses of about 350MPa and load continues to transfer to the {0002} oriented grains and the β-phase. The {0002} grains eventually yield at an applied stress of ~420MPa with the accumulated lattice strain ~8000 microstrain. The load then shifts back to the yielded grains, which produces the second inflection in their stress-strain curves. Qualitatively similar behavior is observed in the direction perpendicular to applied load. Correspondingly, in the β-phase, the stress strain curves of all the three observed grain families shift towards compression when the prismatic α-grains yield. These grains take more and more load and yield once the basal grains in the α phase yield. Due to their lower stiffness and small volume fraction, they develop a larger lattice strain of ~16000 microstrain before yield. The kink back of the {0002} α grains at yield is observed by others and was attributed to the tensile twinning [18], while the big jump of {110} grains close to yield might be caused by the fitting. As shown in Fig. 4b), at a high strain level, the {110} peak is hided totally inside the {10-11} peak, making it difficult to obtain an accurate value.

Figure 7c shows the evolution of intergranular residual strain in α− and β−phases during deformation. Despite the small average residual phase strain in the α−phase (see Fig. 6), large intergranular strains were obtained after 2% macroscopic strain. The grain families, which have a large portion of c-axis component such as {0002} and {10-13}, developed a large compressive residual strain (~$3000\times10^{-6}$), while the others such as {10-10} and {10-11} experience a tensile residual strain (~$1000\times10^{-6}$). Even larger intergranular compression strains were observed in the β-phase after unload. The softer {100} grains have residual strains ~8000-$9000\times10^{-6}$, while grain orientations with {110} and {211} parallel to the loading direction have similar values of close to 5000-$6000\times10^{-6}$. Assuming an average elastic stiffness of α−phase of ~100GPa and β−phase as 80GPa, the residual stresses can be roughly estimated as ~100 to -300 MPa in α−phase and 400-640MPa in the β−phase, which implies that the Bauschinger effect is expected to be evidenced in these highly stressed grains if subsequent tensile test were carried out.

## Summary

The evolution of interphase and intergranular stresses in Zr-2.5Nb was investigated during compression by in-situ TOF neutron diffraction. Load partitioning occurs between grains of the α−phase and also between α− and β−phases. The prismatic grains yield at lower applied

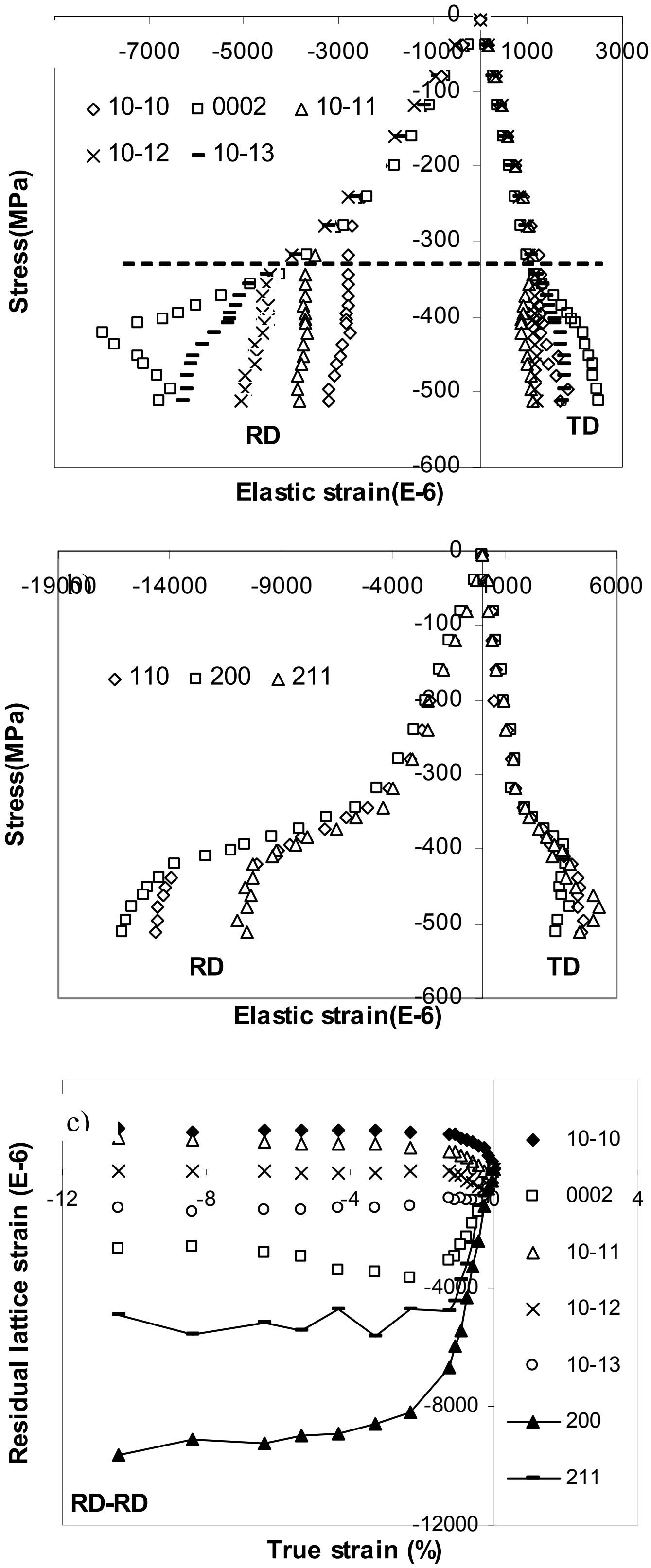


Figure 7 Evolution of lattice strain of selected grain families during compression of RD sample, a) α−phase, b) β− phase, c) intergranular residual strain in the axial direction. Dash lines indicate the macroscopic yield stress. The error is ~20-$50\times10^{-6}$ for α−phase and 100-$200\times10^{-6}$ for β−phase.

stresses. With increasing macroscopic strain, more and more load increment was taken by the basal grains and the β−phase. The basal grains yield at higher applied stresses, transfer load to the β−phase and cause the yield of β−phase. The load is then transferred back to the α−phase causing a second reflection in the stress strain curve. It is the load partitioning that produces the large residual interphase and intergranular stresses in Zr-2.5Nb. The average residual stress is low in the α−phase, however, the intergranular stresses are still very high.

## Acknowledgements

This research is supported by NSERC, COG, OPG and Nu-Tech Precision Metals under the Industrial Research Chair Program in Nuclear Materials at Queen's University. The experiments were carried out at the ISIS pulsed neutron facility at Rutherford Appleton Laboratory, Oxon., UK.

## References

[1] D. G. Hurst et al: *Canada enters the nuclear age* (Montreal & Kingston: McGill-Queen's University press, 1997)
[2] C. N. Tomé, N. Christodoulou: Philos. Mag. A80 (2000), p. 1407
[3] R. A. Holt, N. Christodoulou, A. R. Causey: J. Nucl. Mater. 317 (2003), p.256
[4] C.H. Woo, A. R. Causey, R. A. Holt: Philos. Mag. 79 (1999), p. 59
[5] N. Christodoulou, P. A. Turner, E.T.C. Ho, C. K. Chow, M. Resta levi: Metall. Mater. Trans. A 31 (2000), p. 409
[6] D. X. Du, C. H. Woo: Computational Materials Science 23 (2002), p.260
[7] T. W. Clyne, P. J. Withers: *An Introduction to Metal Matrix Composites* (Cambridge: Cambridge University press; 1993).
[8] P. J. Withers, A. P. Clarke: Acta Mater. Vol. 46 (1998), p. 6585
[9] E. C. Oliver, M. R. Daymond, P.J. Withers: Acta Mater. 52 (2004), p. 1937
[10] M. R. Daymond, C. Hartig, H. Mecking: Acta Mater. 53 (2005), p. 2805
[11] V. Randle: *Introduction to Texture Analysis* (Amsterdam, The Netherlands : Gordon and Breach Science Publishers, 2000)
[12] M.R. Daymond, M. A. M . Bourke, R. B. Von Dreele, B. Clausen, T. Lorentzen: J. Appl. Phys. 82 (1997), p. 1554
[13] M.R. Daymond, M. A. M . Bourke, R. B. Von Dreele: J. Appl. Phys. 85 (1999), p. 739
[14] R. A. Holt and E. F. Ibrahim: Acta Metallurgica, 27 (1979), p. 1319
[15] M. R. Daymond, H. G. Priesmeyer: Acta Mater. 50 (2002), p. 1613
[16] http://www.isis.rl.ac.uk/engineering
[17] G. Aurelio, A. Fernandez Guillermet, G. J. Culleo, J. Campo: Metall. Mater. Trans. A 34 (2003), p. 2771
[18] F. Xu, R.A. Holt, E.C. Oliver and M.R. Daymond: In process.